Journal of Engineering Research and Reports

23(10): 57-66, 2022; Article no.JERR.92921
ISSN: 2582-2926

Obtaining Pedestrian Interest Regions Using Experimental Methods

Bo Zhang [a*] and Denghui Liu [a]

[a] School of Civil Engineering and Ttransportation, North China University of Water Resources and Hydropower, Zhengzhou 450045, China.

Authors' contributions

This work was carried out in collaboration among both authors. Both authors read and approved the final manuscript.

Article Information

DOI: 10.9734/JERR/2022/v23i10752

Open Peer Review History:
This journal follows the Advanced Open Peer Review policy. Identity of the Reviewers, Editor(s) and additional Reviewers, peer review comments, different versions of the manuscript, comments of the editors, etc are available here: https://www.sdiarticle5.com/review-history/92921

Method Article

Received 23 August 2022
Accepted 30 October 2022
Published 05 November 2022

ABSTRACT

In pedestrian simulation, using the region of interest of pedestrians can solve the problem of data redundancy and complexity and lack of representation in the pedestrian saccade range, and establish an efficient pedestrian collision avoidance behavior model. The real-time eye movement data of unidirectional and bidirectional pedestrian flow were collected by eye tracker, and the mathematical models of pedestrian flow density, radius and angle of each region of interest were established. Analyzing the experimental data, it is found that the range of pedestrian interest region is affected by pedestrian density. The angle of the pedestrian interest region is generally not more than 90°, and the radius of the high-interest region and the low-interest region are negatively correlated with the pedestrian density. When the pedestrian density reaches a certain degree, the radius of the high-interest region and the low-interest region approach the fixed value respectively.

Keywords: Pedestrian flow; region of interest; eye movement behavior.

1. INTRODUCTION

The complexity of pedestrian behavior comes from the existence of collective behavior mode, which is evolved from the interaction between a large number of individuals within a certain range. Therefore, building an effective range of pedestrian interaction becomes a key point of pedestrian flow model.

**Corresponding author: Email: 2461841980@qq.com;*

However, the range of pedestrian interaction in different models is different. In the discrete model, such as cellular automata model, the pedestrian interaction range is represented in the form of neighborhood, which is defined by using rules such as Von Neumann type, Moore type and extended Moore type (Fig.1). In literature [1,2,3], the neighborhood is the distance of one cell in four directions (Fig.1(a)). In literature [4,5,6], the neighborhood is the distance of one cell in eight directions (Fig.1(b)). Reference [7] expands the neighborhood to a larger scope (Fig.1(d)). These completely depend on the type of neighborhood, ignoring the impact of individual vision and other differential physiological characteristics on the pedestrian interaction range. Literature [8,9] take a fixed number of the nearest pedestrians as the interaction range based on K-nearest neighbor topology (Fig.1(e)). The influence of dynamic information of neighbor on individual motion is emphasized, while the effect of static information such as surrounding obstacles and buildings on pedestrians is ignored. Reference [10,11] introduced the circle of interaction radius to represent the consideration of the surrounding environment (Fig.1(f)). When the cell division is not precise, the boundary of pedestrian interaction will be unclear. In continuous models, such as social force model and heuristic model, there are two typical pedestrian interaction ranges. Reference [12,13] introduced the circle of interaction radius to represent the consideration of the surrounding environment (Fig.1(g)). Literature [14,15,16] considered visual information, set a sector area around a single pedestrian, and define its radius and angle (Fig.1(h)). However, these models assume a certain area as the pedestrian interaction range, and rarely have been calibrated and verified on the validity of real data and parameter details.

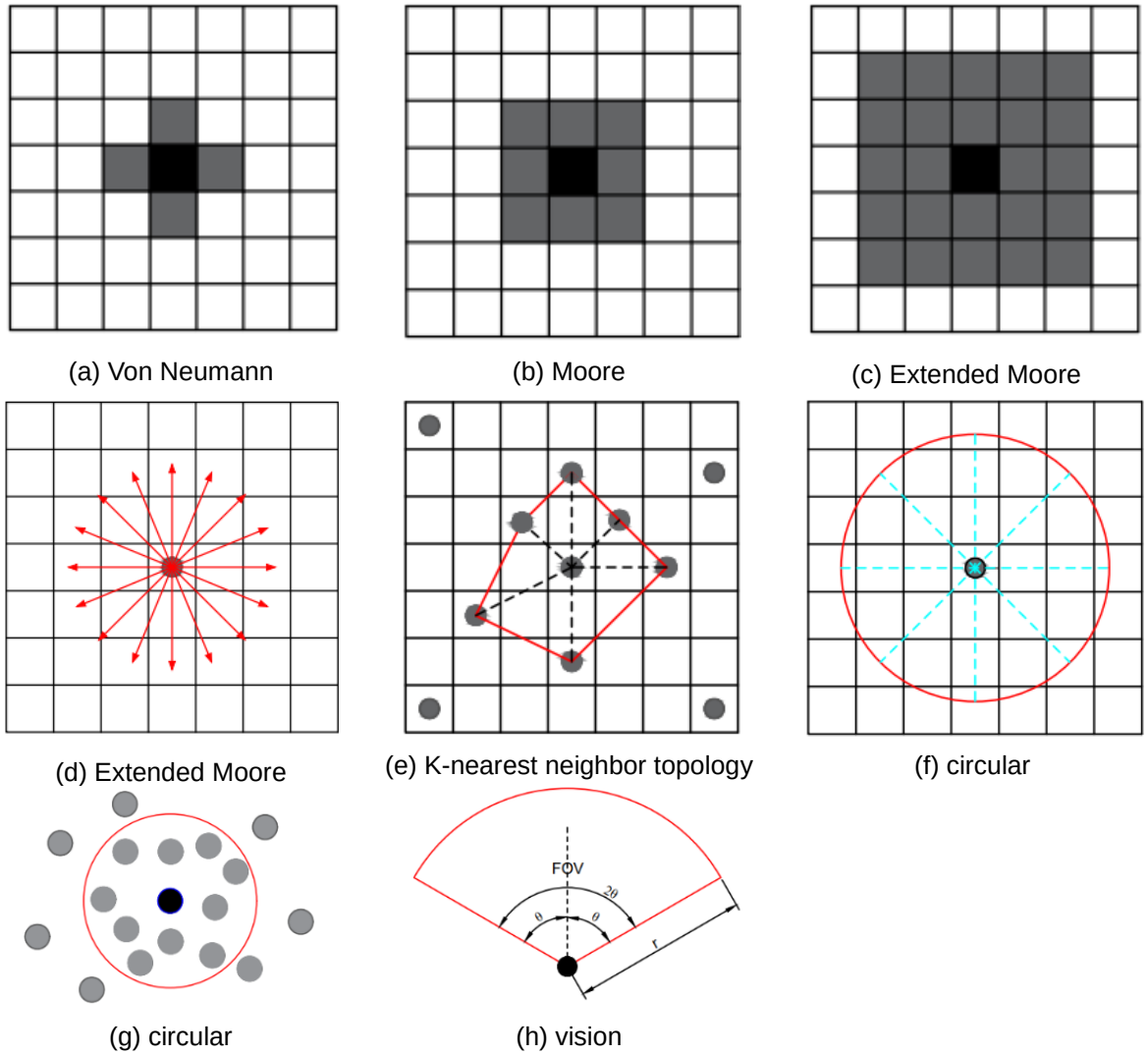

(a) Von Neumann (b) Moore (c) Extended Moore

(d) Extended Moore (e) K-nearest neighbor topology (f) circular

(g) circular (h) vision

Fig. 1(A-H). Range of pedestrian interaction in different models

In practical situations, pedestrians do not care about the global information in the moving scene, but only pay attention to the local area information that they are interested in. Pedestrian interest points are usually points with rich content and high information content. These points are the most representative points in the motion scene. From this, it can be obtained that the interest region composed of interest points also has high information content. Therefore, instead of considering the global information of the moving scene, only the local area information of interest to pedestrians is extracted. In order to establish an effective range of pedestrian interaction, this paper proposes a method to obtain pedestrian interest regions. Based on the pedestrian eye movement behavior experiment, the pedestrian interest region is divided. The pedestrian interest region maintains the basic shape of the pedestrian interaction area, making the boundary of the pedestrian interaction area clear, without the phenomenon of unclear demarcation of the pedestrian interaction boundary, and taking into account the impact of different physiological features such as vision on the pedestrian interest region.Considering how one-way and two-way pedestrian flows, which are common in daily life and have different densities, affect the range of pedestrian interest regions, a mathematical model of one-way and two-way pedestrian flow density and the radius and angle of each interest region is established.The research on the pedestrian region of interest provides data support and theoretical guidance for the development of pedestrian simulation collision avoidance algorithms with different densities, thereby helping to further improve the pedestrian simulation model.

2. EXTRACTION METHOD OF PEDESTRIAN INTEREST REGION

In this paper, the eye tracker is mainly used to collect real-time data of eye movement behavior of participants, which allows the establishment and research of virtual environment, which is impossible to reproduce in the real world. Firstly, the pedestrian movement scene information was collected by simultaneously recording the pedestrian flow video at the horizontal and overlooking level. Secondly, the eye tracker was used to obtain the eye movement behavior data information related to gaze intensity, such as gaze frequency and gaze duration. Then, interest points were extracted by time threshold method and outliers were eliminated. Finally, the pedestrian attention formula is introduced to measure the stimulation degree of static and dynamic factors to pedestrians, and the different division of interest regions is realized by clustering internal filling.

2.1 Pedestrian Interest Point Extraction

Pedestrian interest points are usually points with rich and high amount of information. These points are the most representative points in the pedestrian motion scene. They are points that select useful information from a large number of information and guarantee the effectiveness of pedestrian walking perception process. Research shows that human eyeballs mainly have three basic forms of movement: fixation, saccade and smooth tracking 17. Look at the behavioral movement to locate and observe the content you are interested in, and the duration is between 100ms-1200ms. If the gaze exceeds 1200ms, it is considered to be dazed. The saccade behavior movement is that the fixation point position jumps quickly from one observation area to the next. Smooth tracking motion means that when the pedestrian's head remains stationary, in order to keep the fixation point always on the observation object, the eyes should follow the observation object to make compensation motion. In this paper, we use the time threshold method to extract the points of interest. When the participants' fixation time on a point exceeds the threshold value T_i, the fixation point is considered as the point of interest. As shown in the Fig. 2, the blue aperture in the figure represents the fixation point of pedestrians. If the fixation time of the fixation point exceeds the time threshold T_i, the fixation point is considered as the point of interest. If the point of interest of the next frame falls on the same object and is within 3 ° from the axis to the original gaze position, it is considered to gaze at the same point of interest. In this paper, if a pedestrian gazes at the same point for more than three consecutive frames, the fixation point is considered as an interest point.

2.2 Pedestrian Interest Region Extraction

The pedestrian interest region is composed of the current pedestrians and interest points, but it is impossible to fully understand the scope of the pedestrian interest region, even with the most advanced neuroscience 18. In order to simplify the experiment, the region of interest is composed of three parameters: interest level, radius and angle. Referring to literature 19, the region of interest is divided into high interest region (ROI0), low interest region (ROI1) and no

interest region (ROI2) (Fig.3(i)). This paper mainly studies regions of high interest and regions of low interest. In order to divide regions of interest, attention formula is introduced to measure the stimulation degree of static and dynamic factors on pedestrians. con (p, i) is used to represent the attention paid by participants to interest point i at the current position of pedestrian p, and the calculation formula is as follows:

$$\mathrm{con}(p,\ i) = \frac{N(p,\ i)}{N(I)} \times \frac{N(i,p)}{N(P)} \quad (1)$$

N (p, i) represents the frequency of the participants' gaze at the interest point i at the current pedestrian p position, N (I) represents the total interest point frequencies of the participants at the current pedestrian p position, N (i, p) represents the number of people at the interest point i, and N (p) represents the total number of participants.

Fig. 2. An eye tracker tests a frame in a video sequence

If participants pay the highest attention to a point of interest in consecutive frames, they are considered as high interest points . Taking the distance from the position of the high interest point in the first frame to the pedestrian at the current position as the radius of the high interest region r_1, the maximum distance from all the interesting points of the participants to the pedestrian at the current position as the radius of the low interest region r_2. The maximum angle formed by two points of all interest points in the continuous frame number of participants and pedestrians in the current position is the angle θ of the interest region.In the process of interest point detection, some points are not regarded as interest points, but these points are actually part of the interest region, and can be regarded as interest points by the method of inner filling. As shown in Fig. 3(j), the interest points of the participants at the current position of pedestrian p are a, b, c, d, e, f, and pedestrian b is the high interest point of the participants, then the distance from the position of pedestrian p to the point of interest b is recorded is the radius r_1 of the high interest region, the distance from the position of the pedestrian p to the interest point f is recorded as the low interest region radius r_2, and the angle of the interest region is the angle θ between the interest points a and c and the current row p. The unlabeled pedestrians g and h in the figure are non interest points, but the components of interest regions are filled in as interest points by clustering. If the centers of pedestrians i and j are not within the region of interest, they are non interest points and will not be considered.

3. EXPERIMENT AND ANALYSIS

3.1 Experimental Design

This experiment is divided into two parts: pedestrian movement scene information collection and eye movement behavior data collection.

In the pedestrian movement scene information collection experiment, horizontal and overlooking video of pedestrian flow are simultaneously recorded (Fig. 4(k),(l)). The horizontal and overhead recordings were made with a head-mounted camera and a hand-held camera, respectively, with a frame rate of 30 frames. The experimental site is the hall on the first floor of a teaching building in a university, and the shooting time is when students go to and from class. The floor tile size is 600×600mm, which can well realize video recording of pedestrian flow with different densities and distance estimation between pedestrians.

The pedestrian density of high interest region and low interest region is taken as the pedestrian flow density. The formula for calculating the parameters of the region of interest is as follows (Fig. 5):

The radii of the regions of high interest and low interest are calculated as follows:

$$r_1 = \sqrt{a^2 + b^2} \qquad r_2 = \sqrt{c^2 + d^2} \quad (2)$$

The angle of the region of interest is calculated according to the following formula:

$$\theta_1 = \sin^{-1}\frac{k}{r_1}\ \theta_2 = \tan^{-1}\frac{a}{b}\ \theta_3 = \tan^{-1}\frac{c}{d}\ \ \theta_4 = \sin^{-1}\frac{k}{r_2} \qquad \theta = \theta_1 + \theta_2 + \theta_3 + \theta_4 \quad (3)$$

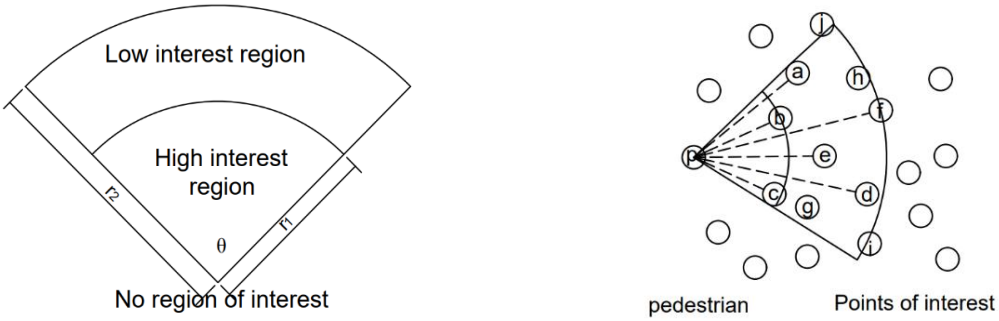

(i) (j)

Fig. 3. (i) Division of regions of interest, (j) Regions of interest extraction

(k) (l)

Fig. 4. (k) Shoot a frame in the scene horizontally, (l) Shoot a frame in a video sequence from the top

Assuming that the high interest point of pedestrian A is interest point B, and the interest point of the maximum distance from pedestrian A is interest point C, where r1 is the radius of the high interest region and r_2 is the radius of the low interest region. a and b represents the horizontal distance and vertical distance from pedestrian A to point of interest B respectively. c and d are the lateral and longitudinal distances of the maximum distance between interest point C and pedestrian A. θ is the Angle between pedestrian A and interest points B and C. K is the radius of personnel body shape, which is 0.2m.

Eye movement behavior data collection experiment (Fig. 2), a total of 30 people participated in the experiment, including 15 females and 15 males, all of whom were college students, and all of them had normal vision or corrected to normal vision. The experimental site was a laboratory, and the experimental equipment was Tobii Eye Tracker 5. In order to prevent the psychological impact of the participants, it was ensured that the participants had not seen the video in advance, and the participants were not given any observation task. Each time the participant changes, the eye tracker needs to be recalibrated. Five videos were recorded, each 25 seconds long. If the eye tracker is used for too long, the experimenter will suffer from cognitive fatigue 20. For the collection of eye-movement behavior data of participants, each video needs to be preheated for 5 seconds. When the interest point of the participants appeared, the first frame of the interest point and the following 20 consecutive frames were taken, and the attention of the 30 participants to the interest point in the 20 consecutive frames was calculated by formula (1). Then, the parameter data of pedestrian interest region can be obtained by calculating equations (2) and (3).

3.2 Analysis of Experimental Data

We collected the eye movement data of 30 participants and obtained 90,000 frames of eye movement behavior data. Through the processing of interest points and calculation of attention, the division of interest regions is realized. Through equations (1), (2) and (3), the parameter data of the pedestrian interest region of 180 groups of unidirectional and bidirectional pedestrian flow under different densities are obtained. Thus, the relationship diagram

between different densities of unidirectional and bidirectional pedestrian flow and the region of interest is obtained, where x represents the density and y represents the radius.

In the one-way pedestrian flow, the fitting function and goodness were obtained by nonlinear fitting to the data of different densities and radii of each region of interest (Fig. 6(m)). The fitting function of the pedestrian density and the radius of the region of low interest is $y = 3.2988x^{-0.58}$, and the goodness of fit R^2=0.8025. The fitting function of the pedestrian density and the radius of the region of high interest is $y = 1.6869x^{-0.505}$, and the goodness of fit R^2=0.5537. According to the fitted curve, it is found that the radius of the region of interest changes with the change of the pedestrian density. The radius of each region of interest does not always change with the change of pedestrian density. When the pedestrian density approaches the saturation value, the radius of each region of interest tends to a fixed value. Here, the threshold value of pedestrian density is 6p/m^2. When the pedestrian density is less than 6p/m^2, the radius of high-interest and low-interest regions of pedestrians decreases with the increase of density. When the pedestrian flow density is greater than 6p/m^2, the radius of the high-interest region tends to a fixed value of 0.7m, and the radius of the low-interest region tends to be 1m. The radius of high interest region and low interest region of pedestrians are mainly between 0.7-1.7m and 1.7-3.8m, respectively. The angle distribution of the region of interest ranged from 36° to 88°, mainly from 40° to 80°.

In the bidirectional pedestrian flow, the fitting function and goodness were obtained by nonlinear fitting to the data of different densities and radii of each region of interest (Fig. 7(o)). The fitting function of the pedestrian density and the radius of the region of low interest is $y = 3.2231x^{-0.439}$, and the goodness of fit R^2=0.5481. The fitting function of the pedestrian density and the radius of the region of high interest is $y = 1.8269x^{-0.323}$, and the goodness of fit R^2=0.303. According to the fitted curve, it is found that the radius of the region of interest changes with the change of the pedestrian density. The radius of each region of interest does not always change with the change of pedestrian density. When the pedestrian density approaches the saturation value, the radius of each region of interest tends to a fixed value. Here, the threshold value of pedestrian density is 6p/m^2. When the pedestrian density is less than 6p/m^2, the radius of high-interest and low-interest regions of pedestrians decreases with the increase of density. When the pedestrian density is greater than 6p/m^2, the radius of the high-interest region tends to the fixed value of 1m, and the radius of the low-interest region tends to the fixed value of 1.3m. The radius of high interest region and low interest region of pedestrians are mainly between 1.0-2.2m and 2.2-4.0m, respectively. The angle distribution of the region of interest ranged from 35° to 87°, mainly from 40° to 70°.

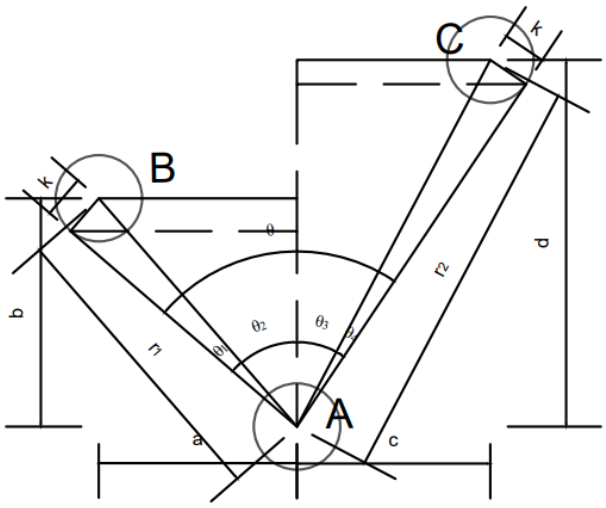

Fig. 5. Calculation of ROI parameters

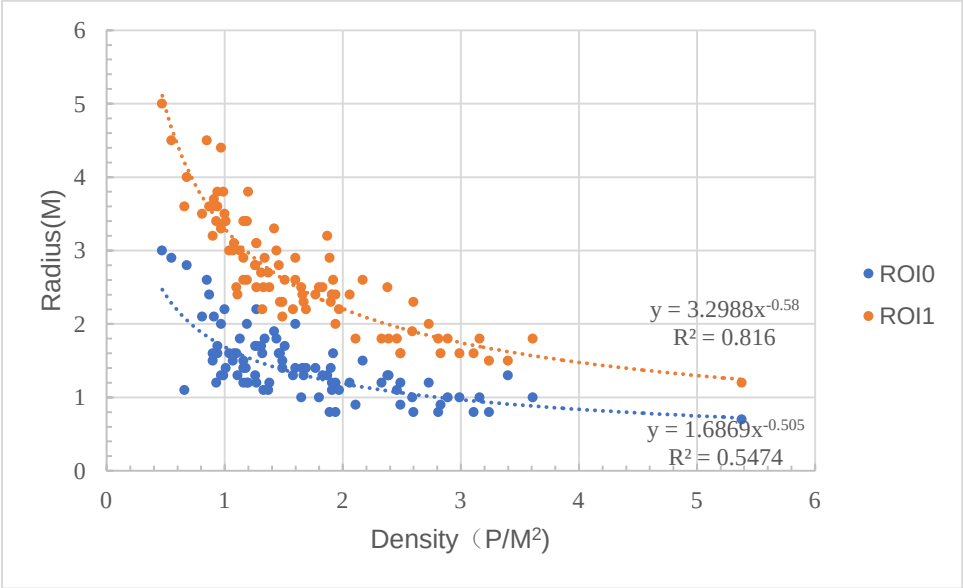

(m)

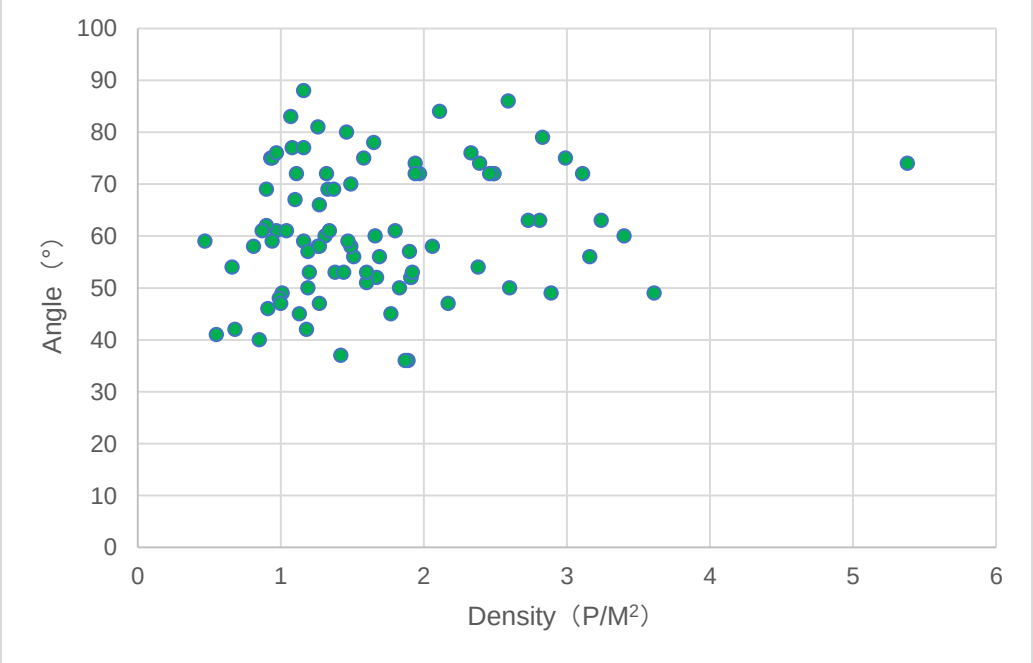

(n)

Fig. 6. (m) The relationship between one-way pedestrian flow density and the radius of each region of interest,(n) The relationship between one-way pedestrian flow density and the angle of region of interest

According to the fitted curve, it is found that the region of interest of pedestrians changes with the density of pedestrian flow. Therefore, a single fixed range cannot be used to represent the interaction range of pedestrians in the pedestrian flow model. With the increase of pedestrian density, the radius of high interest region and low interest region of pedestrians decreases, that is, the radius of interest region is negatively correlated with pedestrian density. When the pedestrian density reaches a certain degree, the radius of the region

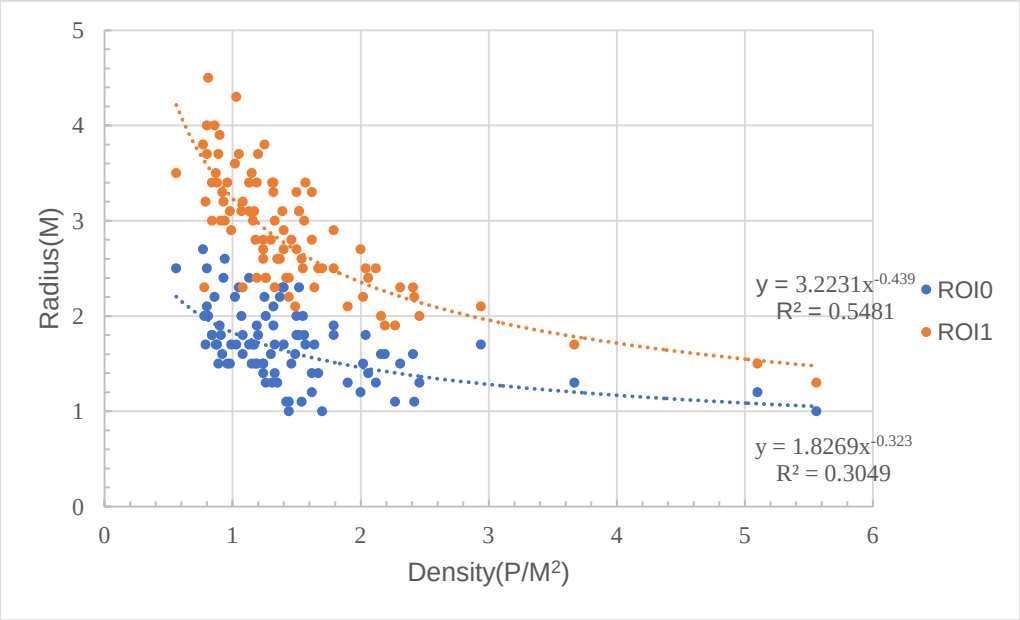

(o)

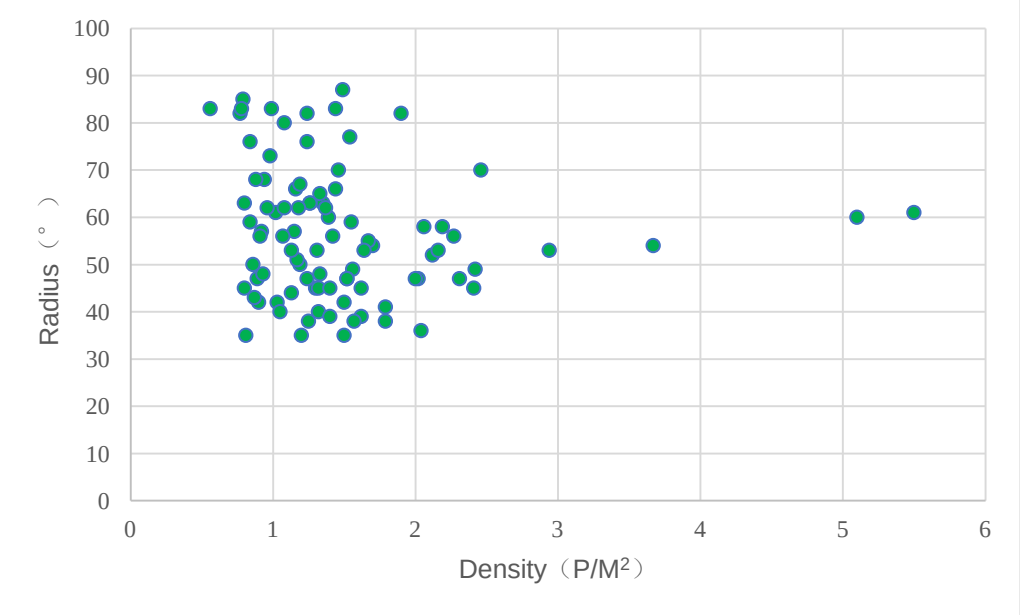

(p)

Fig. 7. (o) The relationship between the density of two-way pedestrian flow and the radius of each region of interest, (p) The relationship between two-way pedestrian flow density and the angle of region of interest

of high interest and the region of low interest tend to a fixed value respectively. The fitting function is not absolute, it just represents a trend. Discrete points are distributed around the fitted curve, indicating that the radius of the pedestrian interest region is variable, which is less than or greater than the fitted value, but the specific value should be determined according to the surrounding environment.

4. CONCLUSION

In order to establish an effective pedestrian interaction range, this paper proposes a method to obtain the pedestrian interest region. The eye movement data of unidirectional and bidirectional pedestrian flow under different densities were analyzed by eye tracker, and the different divisions of pedestrian interest regions were realized. The influence of pedestrian flow density on the region of interest was explored, and the mathematical models of unidirectional and bidirectional pedestrian flow and the radius and Angle of the region of interest under different densities were established. The following conclusions are obtained:

(1) Pedestrian interest region is affected by pedestrian density. Under one-way pedestrian flow, the relationship between the radius of high interest region and low interest region of pedestrians and pedestrian density is $y = 1.6869x^{-0.505}$ and $y = 3.2988x^{-0.58}$, respectively. In the two-way pedestrian flow, the relationship between the radius of high interest region and low interest region of pedestrians and pedestrian density is $y = 1.8269x^{-0.323}$ and $y = 3.2231x^{-0.439}$, respectively. The radii of high interest region and low interest region of unidirectional and bidirectional pedestrian flow are negatively correlated with pedestrian flow density. The angle of the area of interest for pedestrians generally does not exceed 90°.

(2) The influence trend of unidirectional and bidirectional pedestrian density on the region of interest of pedestrians is the same, but when the density reaches a certain degree, the radius of each region of interest approaches different fixed values. When the pedestrian flow density does not exceed 6p/m^2, the radius of the region of interest decreases with the increase of pedestrian flow density. When the pedestrian flow density exceeds 6p/m^2, the radii of high and low interest regions of one-way pedestrian flow tend to be fixed values of 0.7m and 1m respectively, and the radii of high and low interest regions of two-way pedestrian flow tend to be fixed values of 1m and 1.3m respectively.

(3) In unidirectional pedestrian flow, the radius of high interest region is concentrated between 0-1.7m, and the radius of low interest region is concentrated between 1.7-3.8m, and the angle change is concentrated between 40° and 80°. In bidirectional pedestrian flow, the radius of high-interest region is concentrated between 0-2.2m, and the radius of low-interest region is concentrated between 2.2-4.0m, and the angle change is concentrated between 40° and 70°.

The pedestrian interest region maintains the basic shape of the pedestrian interaction range, making the boundary of the pedestrian interaction range clear and avoiding the phenomenon of unclear boundary. Moreover, the influence of different physiological characteristics such as vision on the pedestrian interest region is taken into account. The pedestrian interest region is obtained through the pedestrian eye movement behavior experiment, which provides data support and parameter calibration for pedestrian flow simulation, rather than assuming a certain region as the pedestrian interaction range. As pedestrian simulation becomes more and more complex, the use of pedestrian interest region can solve the problem of data redundancy and complexity and lack of representation in the pedestrian saccade range, which is helpful to show collision avoidance behavior in pedestrian simulation more complex, and establish an efficient pedestrian collision avoidance behavior model. The influencing factors of the pedestrian interest region are various, so it is necessary to further study the pedestrian interest region. In the future work, we will continue to improve the extraction method of pedestrian interest region to improve the accuracy and robustness of the model. The study of pedestrian interest region will be extended to multidirectional flow, and the interest region will be applied to pedestrian simulation model.

COMPETING INTERESTS

Authors have declared that no competing interests exist.

REFERENCES

1. Jian L, Lizhong Y, Daoliang Z. Simulation of bi-direction pedestrian movement in corridor [J]. Physica A: Statistical Mechanics and its Applications. 2005; 354:619-628.
2. Weng W G, Chen T, Yuan H Y, et al. Cellular automaton simulation of pedestrian counter flow with different walk velocities [J]. Physical Review E. 2006; 74(3):036102.
3. Zhou X, Hu J, Ji X, et al. Cellular automaton simulation of pedestrian flow considering vision and multi-velocity[J]. Physica A: Statistical Mechanics and its Applications. 2019;514:982-992.

4. Zou B, Lu C, Mao S, et al. Effect of pedestrian judgement on evacuation efficiency considering hesitation [J]. Physica A: Statistical Mechanics and its Applications. 2020;547:122943.
5. Xiao Q, Li J. Evacuation model of emotional contagion crowd based on cellular automata [J]. Discrete Dynamics in Nature and Society; 2021.
6. Li B, Hou J, Ma Y, et al. A coupled high-resolution hydrodynamic and cellular automata-based evacuation route planning model for pedestrians in flooding scenarios [J]. Natural hazards. 2022;110(1):607-628.
7. Huo F, Li Y, Li C, et al. An extended model describing pedestrian evacuation considering pedestrian crowding and stampede behavior [J]. Physica A: Statistical Mechanics and its Applications. 2022;604:127907.
8. Ballerini M, Cabibbo N, Candelier R, et al. Interaction ruling animal collective behavior depends on topological rather than metric distance: Evidence from a field study [J]. Proceedings of the National Academy of Sciences. 2008;105(4):1232-1237.
9. Ma J, Song W, Zhang J, et al. k-Nearest-Neighbor interaction induced self-organized pedestrian counter flow [J]. Physica A: Statistical Mechanics and its Applications. 2010;389(10):2101-2117.
10. Cao S, Qian J, Li X, et al. Evacuation simulation considering the heterogeneity of pedestrian under terrorist attacks [J]. International Journal of Disaster Risk Reduction. 2022;79:103203.
11. Li S, Niu H. Simulation of bi-direction pedestrian movement in corridor based on crowd space [J]. Procedia-social and behavioral sciences. 2014;138:323-331.
12. Wu W, Chen M, Li J, et al. An extended social force model via pedestrian heterogeneity affecting the self-driven force [J]. IEEE Transactions on Intelligent Transportation Systems; 2021.
13. Chraibi M, Seyfried A, Schadschneider A. Generalized centrifugal-force model for pedestrian dynamics[J]. Physical Review E. 2010;82(4):046111.
14. Ma L, Chen B, Wang X, et al. The analysis on the desired speed in social force model using a data driven approach [J]. Physica A: Statistical Mechanics and its Applications. 2019;525:894-911.
15. Jia X, Yue H, Tian X, et al. Simulation of pedestrian flow with evading and surpassing behavior in a walking passageway [J]. Simulation. 2017;93(12): 1013-1035.
16. Corbetta A, Meeusen J A, Lee C, et al. Physics-based modeling and data representation of pairwise interactions among pedestrians[J]. Physical review E. 2018;98(6):062310.
17. Andrews T J, Coppola D M. Idiosyncratic characteristics of saccadic eye movements when viewing different visual environments [J]. Vision research. 1999;39(17):2947-2953.
18. Fujiyama T. Investigating density effects on the" awareness" area of pedestrians using an eye tracker [J]; 2006.
19. Morini F, Yersin B, Maïm J, et al. Real-time scalable motion planning for crowds [C]. International Conference on Cyberworlds (CW'07). IEEE, 2007:144-151.
20. Van der Hulst M, Meijman T, Rothengatter T. Maintaining task set under fatigue: A study of time-on-task effects in simulated driving [J]. Transportation Research Part F: Traffic Psychology and Behavior. 2001; 4(2):103-118.

Peer-review history:
The peer review history for this paper can be accessed here:
https://www.sdiarticle5.com/review-history/92921